

Permutation Enhanced Parallel Reconstruction with A Linear Compressive Sampling Device

Hao Fang, Sergiy A. Vorobyov, and Hai Jiang

Abstract

In this letter, a permutation enhanced parallel reconstruction architecture for compressive sampling is proposed. In this architecture, a measurement matrix is constructed from a block-diagonal sensing matrix and the sparsifying basis of the target signal. In this way, the projection of the signal onto the sparsifying basis can be divided into several segments and all segments can be reconstructed in parallel. Thus, the computational complexity and the time for reconstruction can be reduced significantly. This feature is especially appealing for big data processing. Furthermore, to reduce the number of measurements needed to achieve the desired reconstruction error performance, permutation is introduced for the projection of the signal. It is shown that the permutation can be performed implicitly by using a pre-designed measurement matrix. Thus, the permutation enhanced parallel reconstruction can be achieved with a linear compressive sampling device.

Index Terms

Compressive sampling, parallel reconstruction, permutation.

I. INTRODUCTION

In compressive sampling (CS), a signal \mathbf{x} can be compressed using a *measurement matrix* Φ , which results in a measurement vector $\mathbf{y} = \Phi\mathbf{x}$ whose length is significantly smaller than that of \mathbf{x} . If the projection θ of \mathbf{x} onto an orthonormal basis Ψ is sparse, then θ , and thus \mathbf{x} , can be reconstructed from \mathbf{y} [1], [2]. This recoverability is guaranteed by the restricted isometry property (RIP) on the *sensing matrix* $\mathbf{A} \triangleq \Phi\Psi$. Obviously, the measurement vector \mathbf{y} can be also obtained from \mathbf{A} and θ as $\mathbf{y} = \mathbf{A}\theta$.

S. A. Vorobyov is the corresponding author. The authors are with the Department of Electrical and Computer Engineering, University of Alberta, Edmonton, AB, T6G 2V4, Canada; e-mail: {hfang2, svorobyov, hail}@ualberta.ca.

It is known that the CS reconstruction process has very high computational complexity. Although using a block-diagonal measurement matrix Φ can make parallel reconstruction of signal \mathbf{x} 's segments possible, the error performance degrades compared to using a centralized reconstruction scheme [3]–[5]. Recently, a permutation enhanced parallel sampling and parallel reconstruction architecture has been proposed for CS in [6], [7], where segments of sparse projection θ (not the signal \mathbf{x}) are sampled and reconstructed in parallel. In [7], the sparse projection θ is reshaped into a 2D matrix and permuted. All columns of the permuted 2D matrix are then sampled in parallel. While the reshaping operation leads to parallel reconstruction and the permutation operation improves the error performance of parallel reconstruction, the non-linearity introduced by these operations at the encoder side makes it difficult to implement the sampling device at a linear system. To address the above problem, we propose in this letter a way to preserve the linearity of the encoder. It is shown that the permutation enhanced parallel reconstruction can be still applied without affecting the linearity at the encoder side.

In the proposed architecture, a block-diagonal sensing matrix \mathbf{A} is employed, and the measurement matrix Φ for the encoder is constructed as $\Phi = \mathbf{A}\Psi^T$ where $(\cdot)^T$ denotes the transpose operation. This is different from the architectures in [3]–[5] where a block-diagonal measurement matrix Φ is used and the sensing matrix \mathbf{A} for the decoder is constructed based on Φ and Ψ . With a block-diagonal sensing matrix, different segments of the projection θ can be reconstructed in parallel, which helps to significantly reduce the computational complexity and the time needed in reconstruction. Furthermore, we show that if a permutation that improves the reconstruction error performance is applied on θ , the corresponding measurements \mathbf{y}^\dagger can be obtained by multiplying the signal \mathbf{x} with a new measurement matrix Φ^\dagger . In this proposed architecture, the projection θ is not required to be reshaped and explicitly permuted at the encoder side, and thus, it avoids the non-linearity at the encoder side. This nice property enables the implementation of the CS sampling device for the permutation enhanced parallel reconstruction as a linear system such as the single-pixel camera [8].

II. PERMUTATION ENHANCED PARALLEL RECONSTRUCTION FOR CS

A. Parallel reconstruction

In this letter, we consider the general case of a multidimensional signal $\mathbf{x} \in \mathbb{R}^{N_1 \times \dots \times N_d}$. The vector-reshaped representation of \mathbf{x} is $\bar{\mathbf{x}} \in \mathbb{R}^{\bar{N}}$ where $\bar{N} = \prod_{i=1}^d N_i$. Let the projection of $\bar{\mathbf{x}}$ on an orthonormal sparsifying basis $\bar{\Psi} \in \mathbb{R}^{\bar{N} \times \bar{N}}$ be $\bar{\theta}$, i.e., $\bar{\mathbf{x}} = \bar{\Psi}\bar{\theta}$. The sparsifying basis $\bar{\Psi}$ can be obtained by the Kronecker product of several sparsifying bases corresponding to different dimensions, and thus the orthonor-

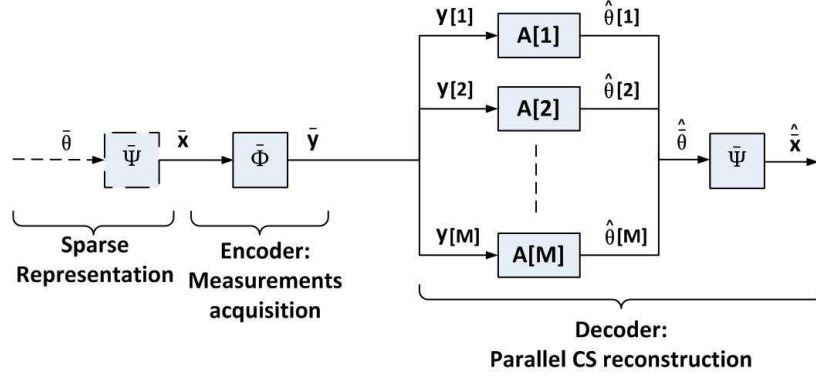


Fig. 1: Block diagram of the system employing the parallel CS reconstruction architecture.

mality preserves [5]. Hence, the measurement vector for \bar{x} can be obtained by $\bar{y} = \bar{\Phi}\bar{x} = \bar{\Phi}\bar{\Psi}\bar{\theta} = \bar{A}\bar{\theta}$ where $\bar{\Phi}$ is the measurement matrix and $\bar{A} \triangleq \bar{\Phi}\bar{\Psi}$ is the sensing matrix. The decoder needs to reconstruct $\bar{\theta}$ from $\bar{y} = \bar{A}\bar{\theta}$.

In the parallel CS reconstruction architecture proposed in this letter, our objective is to design the sensing matrix \bar{A} such that different segments of $\bar{\theta}$ can be reconstructed in parallel. We partition $\bar{\theta}$ into M segments such that

$$\bar{\theta} = [\underbrace{\theta_1 \cdots \theta_{l_1}}_{\theta^x[1]} \underbrace{\theta_{l_1+1} \cdots \theta_{l_1+l_2}}_{\theta^x[2]} \cdots \underbrace{\theta_{l_1+l_2+\cdots+l_{M-1}+1} \cdots \theta_{\bar{N}}}_{\theta^x[M]}]^T$$

where θ_i denotes the i -th element of signal $\bar{\theta}$, and $\theta^x[i]$ denotes the i -th segment with length l_i of signal $\bar{\theta}$. So we have $\bar{N} = \sum_{i=1}^M l_i$. Besides, we design the sensing matrix of size $K \times \bar{N}$ as a block-diagonal matrix, i.e., $\bar{A} = \text{diag}(\mathbf{A}[1], \mathbf{A}[2], \dots, \mathbf{A}[M])$, where $\mathbf{A}[i] \in \mathbb{R}^{K_i \times l_i}$ and $\sum_{i=1}^M K_i = K$.

The block diagram of the system employing the parallel CS reconstruction architecture is given in Fig. 1. In practice, during the acquisition of measurements, $\bar{\theta}$ is not required to be obtained and $\bar{\Psi}$ is not required to be stored, which is shown in the diagram by the dashed line and dashed line border of the corresponding block. At the encoder side, the measurement matrix is a pre-designed matrix, which is given by $\bar{\Phi} = \bar{A}\bar{\Psi}^T$, and the measurement vector is given by $\bar{y} = \bar{\Phi}\bar{x}$. At the decoder side, since \bar{A} is block-diagonal, the measurement vector $\bar{y} = \bar{A}\bar{\theta}$ can be divided into M segments, i.e., $y[i] = \mathbf{A}[i]\theta^x[i]$ ($i = 1, 2, \dots, M$) where $y[i]$ denotes the i -th measurement sub-vector. In this way, all segments of $\bar{\theta}$ can be reconstructed in parallel, and the signal can be recovered via $\hat{x} = \bar{\Psi}\hat{\theta}$ where \hat{x} and $\hat{\theta}$ are the reconstructed signal and its projection on corresponding sparsifying basis, respectively. In the block diagram shown in Fig. 1, the block $\mathbf{A}[i]$ represents the i -th CS decoding processor. The inputs of the

CS decoding processors are the measurement sub-vectors $\mathbf{y}[i]$'s and the outputs are the reconstructed segments $\hat{\boldsymbol{\theta}}[i]$'s, which are then stacked in one vector $\hat{\boldsymbol{\theta}}$.

Denote the sparsity level of projection $\bar{\boldsymbol{\theta}}$ as S , i.e., there are only $S \ll \bar{N}$ nonzero entries in $\bar{\boldsymbol{\theta}}$, and denote the sparsity level of $\boldsymbol{\theta}[i]$ as S_i . Thus, $\sum_{i=1}^M S_i = S$. It is known that in order to reconstruct exactly $\boldsymbol{\theta}[i]$, the sensing matrix $\mathbf{A}[i]$ needs to satisfy the RIP condition determined by S_i [9]. Smaller S_i indicates looser RIP condition, and thus K_i , that is, the number of measurements for $\boldsymbol{\theta}[i]$, can be smaller. Therefore, the design of the sensing matrix $\bar{\mathbf{A}}$ depends on the sparsity levels of the $\boldsymbol{\theta}[i]$'s.

B. Computational complexity

We briefly compare the computational complexity of the parallel CS reconstruction architecture with that of the architectures employing centralized reconstruction. Several solvers exist to reconstruct $\bar{\boldsymbol{\theta}} \in \mathbb{R}^{\bar{N}}$ from $\bar{\mathbf{y}} = \bar{\mathbf{A}}\bar{\boldsymbol{\theta}}$, including for example, the basis pursuit (BP) algorithm based on interior point methods that have computational complexity $\mathcal{O}(\bar{N}^3)$ [10]. For multidimensional signals, since \bar{N} can be dramatically large, the reconstruction process becomes rather slow.

For the parallel CS reconstruction architecture in Fig. 1, each decoding processor only needs to reconstruct a segment of the sparse signal $\bar{\boldsymbol{\theta}}$. Thus, the computational complexity of the i -th decoding processor is only $\mathcal{O}(l_i^3)$, and the total computational complexity is $\mathcal{O}(\sum_{i=1}^M l_i^3)$. The total computational complexity is minimized to $\mathcal{O}(\bar{N}^3/M^2)$ when $l_i = l = \bar{N}/M$ for all i . Thus, by using the parallel CS reconstruction architecture, the computational complexity is much lower.

C. Permutation

To ensure that all decoding processors in Fig. 1 have the same configurations, we assume $l_i = l$ and $\mathbf{A}[i] = \mathbf{A}_0$ for all i . Therefore, to reconstruct exactly all $\boldsymbol{\theta}[i]$'s, $i = 1, 2, \dots, M$, \mathbf{A}_0 needs to satisfy the RIP condition determined by $\max_i \{S_i\}$. However, considering the difference of sparsity levels among all $\boldsymbol{\theta}[i]$'s, $i = 1, 2, \dots, M$, the above setting is not efficient because fewer measurements are actually needed for some segments with smaller S_i . This problem can be solved by applying permutation on $\boldsymbol{\theta}$ such that all segments have similar sparsity level. Then, the required number of measurements to achieve a given error performance can be reduced.

Unlike in [7] where the permutation is applied to the 2D-reshaped matrix of $\boldsymbol{\theta}$ through an algorithm-like process, here the permuted projection $\boldsymbol{\theta}^\dagger$ is obtained in terms of a linear transform by simply multiplying $\boldsymbol{\theta}$ with a permutation matrix \mathbf{P}_π defined as follows. For a permutation π of \bar{N} elements: $\{1, \dots, \bar{N}\} \rightarrow \{1, \dots, \bar{N}\}$ with $\pi(i)$ denoting the new index of the original i -th element after the

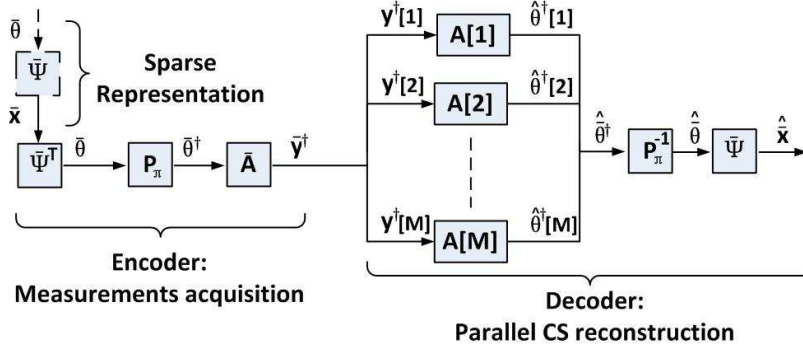


Fig. 2: Block diagram of the system employing the parallel CS reconstruction architecture with permutation on $\bar{\theta}$.

permutation, its permutation matrix is $\mathbf{P}_\pi \in \mathbb{R}^{\bar{N} \times \bar{N}}$, whose entries are all 0 except that the $\pi(i)$ -th entry in the i -th row is 1.

Fig. 2 describes the parallel CS reconstruction architecture with permutation on the projection $\bar{\theta}$. At the encoder side, signal \bar{x} is first projected onto the sparsifying basis $\bar{\Psi}$, which gives the projection $\bar{\theta} = \bar{\Psi}^T \bar{x}$. Then permutation \mathbf{P}_π on the projection $\bar{\theta}$ is applied, which gives the permuted projection $\bar{\theta}^\dagger = \mathbf{P}_\pi \bar{\theta}$. The measurement vector \bar{y}^\dagger of permuted projection $\bar{\theta}^\dagger$ is then given using the sensing matrix $\bar{\mathbf{A}}$ as $\bar{y}^\dagger = \bar{\mathbf{A}} \bar{\theta}^\dagger$. At the decoder side, all segments $\theta^\dagger[i]$ can be reconstructed in parallel from $\mathbf{y}^\dagger[i] = \mathbf{A}[i] \theta^\dagger[i]$ where $\mathbf{y}^\dagger[i]$ and $\theta^\dagger[i]$ are the i -th segment of \bar{y}^\dagger and the i -th segment of $\bar{\theta}^\dagger$, respectively. The inverse permutation is performed after parallel reconstruction of all segments of $\bar{\theta}^\dagger$, i.e., $\hat{\bar{\theta}} = \mathbf{P}_\pi^{-1} \hat{\bar{\theta}}^\dagger = \mathbf{P}_\pi^T \hat{\bar{\theta}}^\dagger$.

Actually, the three blocks representing $\bar{\Psi}$, \mathbf{P}_π , $\bar{\mathbf{A}}$ can be merged into one, which enables to perform the measurements acquisition easily in one step as in most CS sampling devices.

Consider a signal $\bar{x} \in \mathbb{R}^{\bar{N}}$, its projection $\bar{\theta}$ onto the sparsifying basis $\bar{\Psi}$, a sensing matrix $\bar{\mathbf{A}}$, and a permutation matrix \mathbf{P}_π . The measurements acquired in Fig. 2, i.e., $\bar{y}^\dagger = \bar{\mathbf{A}} \bar{\theta}^\dagger$, can also be acquired by sampling \bar{x} directly using a measurement matrix $\bar{\Phi}^\dagger$ given by $\bar{\Phi}^\dagger = \bar{\mathbf{A}} \mathbf{P}_\pi \bar{\Psi}^T$. It straightforwardly follows from the associative law, specifically, $\bar{y}^\dagger = \bar{\mathbf{A}} \bar{\theta}^\dagger = \bar{\mathbf{A}} (\mathbf{P}_\pi \bar{\Psi}^T \bar{x}) = (\bar{\mathbf{A}} \mathbf{P}_\pi \bar{\Psi}^T) \bar{x}$. Therefore, the same measurements \bar{y}^\dagger can be given using a new measurement matrix $\bar{\Phi}^\dagger = \bar{\mathbf{A}} \mathbf{P}_\pi \bar{\Psi}^T$.

Accordingly, the encoder in Fig.2 can be replaced by the encoder shown in Fig.3. Since the new measurement matrix $\bar{\Phi}^\dagger$ is pre-generated and stored at the encoder side, no permutation process is actually required at the encoder side to obtain \bar{y}^\dagger . The only difference between the encoder in Fig. 1 and that in Fig. 3 is the measurement matrix $\bar{\Phi} = \bar{\mathbf{A}} \bar{\Psi}$ in Fig. 1 and the new measurement matrix $\bar{\Phi}^\dagger$ in Fig. 3.

Denote the sparsity level of $\theta^\dagger[i]$ as S_i^\dagger . Recall that we assume $l_i = l$, $\mathbf{A}[i] = \mathbf{A}_0$. If $\max_i \{S_i^\dagger\} <$

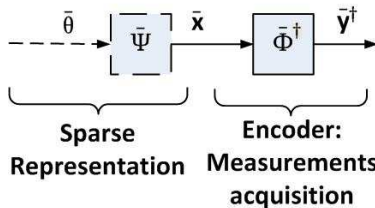


Fig. 3: Equivalent encoder to achieve permutation on $\bar{\theta}$.

$\max_i \{S_i\}$, the required RIP condition for \mathbf{A}_0 to reconstruct $\bar{\theta}^\dagger$ is weaker than that to reconstruct $\bar{\theta}$. Thus, with permutation on $\bar{\theta}$, fewer measurements are needed to achieve the same reconstruction error performance. Note that the exact positions of nonzero entries of $\bar{\theta}$ are not known, and optimal permutation which results in uniform sparsity levels among all segments of $\bar{\theta}^\dagger$ is not practical. Thus, permutation design in practice must be based on a sparsity model of the projection $\bar{\theta}$, for example, as introduced in [7] for video compression application. If no sparsity model is known, the best choice of permutation is a random permutation, which we consider here. Since we assume $l_i = l$, $\bar{\theta}$ can be rewritten as a matrix $\Theta \in \mathbb{R}^{l \times M}$ by letting $\theta[i]$ be the i -th column of Θ . Let C_i be the number of nonzero entries in \mathbf{v}_i , which is the i -th row of Θ . There are $M!$ different permutations that can be applied to \mathbf{v}_i . With a random permutation from the $M!$ possibilities, a nonzero entry in \mathbf{v}_i is permuted to the columns of $1, 2, \dots, M$ with equal probability of $1/M$. Therefore, considering the permuted i -th row, denoted as \mathbf{v}_i^\dagger , the average number of nonzero entries in every column is C_i/M . Assuming that the permutations applied to different rows are independent from each other, the average number of nonzero entries in each column of the resulted matrix is $\sum_{i=1}^l C_i/M$. Therefore, in average, every column of the resulted matrix has the same sparsity level. For example, if the projection $\bar{\theta}$ has length 1000 and we set $l = 100$ and $M = 10$, for a randomly generated sparse signal Θ with $S = 60$ nonzero entries, after random permutation, the mean and standard deviation of the sparsity level of each column of Θ obtained via 10^5 trials are 6 and 2.28, respectively. Therefore, random permutation results in an acceptable sparsity distribution among segments.

D. Discussion on application

In most existing CS acquisition devices, the measurement matrix is pre-generated and stored in the encoder. The decoder “stores” a corresponding sensing matrix for reconstruction. The reconstruction in CS is known to have high computational complexity compared to the sampling process, especially when the dimension of the signal is very large. Thus, when the computational complexity and time for

reconstruction are crucial evaluation criteria and centralized sampling is acceptable, e.g., in real-time video streaming [11], parallel CS reconstruction is very useful.

The single-pixel camera proposed in [8] is one potential application of the parallel CS reconstruction architecture. In the single-pixel camera, the measurements of the image signal $\bar{\mathbf{x}}$ are acquired without digitalization of the analog signal $\bar{\mathbf{x}}$ by high-rate sampling. To implement the measurement matrix, the single-pixel camera uses a digital micromirror device (DMD) array with pre-designed random patterns [8]. However, the DMD array used in the original single-pixel camera can only represent binary values, whereas in the parallel CS reconstruction architecture, the entries of the measurement matrix have more than two values. This issue can be addressed by using more advanced DMD array. Actually, contemporary DMD can produce 1024 grayscale value [12], and thus, a broader class of measurement matrices can be represented by such DMD array.

III. SIMULATION RESULTS

We compare the reconstruction error performance and the reconstruction time among three different schemes: the centralized CS reconstruction, i.e., $M = 1$; the parallel CS reconstruction, i.e., $M \geq 2$, without permutation; and the parallel CS reconstruction with permutation. The reconstruction time includes the sum of reconstruction time of the decoding processors, as well as the average reconstruction time and the worst reconstruction time of the decoding processors.

Our simulations are performed using Matlab on a laptop computer with Intel Dual Core CPU at 2.70 GHz and 8 GB of memory. The sparse projection $\bar{\boldsymbol{\theta}}$ is a random binary sequence of length $\bar{N} = 1200$ with $S = 60$ nonzero entries, which are randomly distributed across the signal. To ensure that all decoding processors have the same configuration, we set $l_i = l$ and $\mathbf{A}[i] = \mathbf{A}_0 \in \mathbb{R}^{K_0 \times l}$ for all i , where $K_0 = K/M$. Entries of \mathbf{A}_0 are drawn from Gaussian ensembles with variance $1/K_0$. The reconstruction algorithm that we use in each decoding processor is the BP algorithm. The goal of our simulation is to show the maximum improvement that can be brought by introducing permutation. So, \mathbf{P}_π is selected to ensure that all segments of $\bar{\boldsymbol{\theta}}^\dagger$ have the same sparsity level, i.e., $S_i^\dagger = S/M$ for all i , although such permutation may not be practical. We set M to 1, 2, 3, 4, 5 and 10. For $M = 1$, the parallel CS reconstruction boils down to the centralized CS reconstruction. In our simulation, we run 500 trials for each combination of (M, K) and average the results over the trails.

Fig.4a and Fig.4b shows the mean square error (MSE) (normalized to the signal energy) of the reconstructed signal in the three aforementioned schemes versus the number of measurements. It can be seen that the MSE for a fixed number of measurements increases as the number of segments M increases.

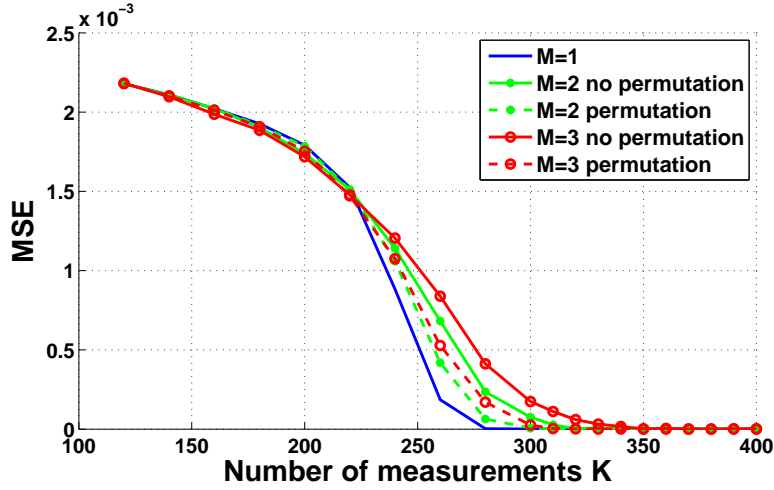
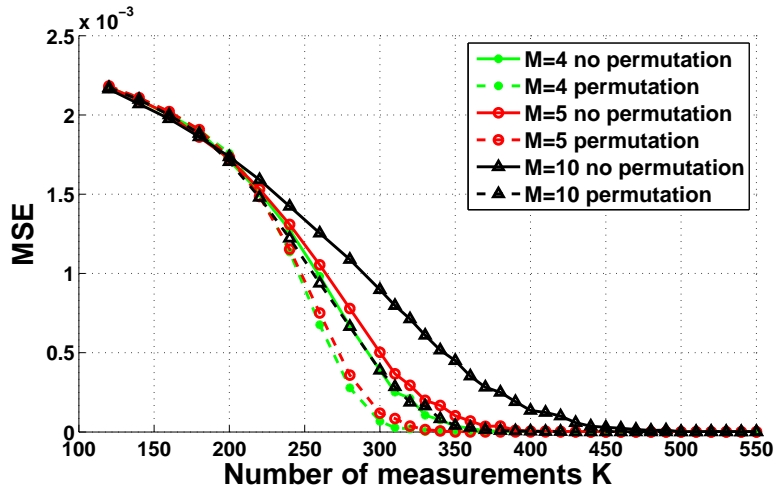
(a) $M = 1, 2, 3$.(b) $M = 4, 5, 10$.

Fig. 4: Reconstruction error performance vs. the number of measurements K for different number of segments M .

In other words, the minimum number of measurements required for exact reconstruction increases as M increases. It is reasonable since the required number of measurements per segment does not linearly decrease when M increases. Besides, it is shown in Fig. 4a and Fig. 4b that for a fixed K , the MSE can be reduced with the permutation. The minimum number of measurements required for exact reconstruction is also reduced with the permutation.

Table I shows the minimum number of measurements and the time required for exact reconstruction.

TABLE I: Minimum number of measurements and reconstruction time (in seconds) required for exact reconstruction.

M	Permutation	K_{require}	t_{total}	t_{average}	t_{worst}
1	N/A	280	4.0243	4.0243	4.0243
2	No	320	1.3946	0.6973	0.7720
2	Yes	300	1.3248	0.6624	0.7290
4	No	370	0.8760	0.2190	0.3041
4	Yes	320	0.8555	0.2139	0.3013
5	No	390	0.9349	0.1870	0.2821
5	Yes	330	0.9132	0.1826	0.2728
10	No	470	1.1799	0.1180	0.1958
10	Yes	370	1.1943	0.1194	0.1992

Here the exact reconstruction is declared if the normalized MSE of the reconstructed signal is smaller than 2×10^{-5} . The total reconstruction time t_{total} is the time used to reconstruct all segments. The average reconstruction time $t_{\text{average}} = t_{\text{total}}/M$ is the average time used to reconstruct each segment. The worst reconstruction time t_{worst} is the maximal reconstruction time used to reconstruct the ‘worst’ segment, given as $t_{\text{worst}} = \max_i \{t_i\}$ where t_i denotes the reconstruction time for the i -th segment. From Table I, the total reconstruction time decreases as M increases from 1 to 4. When M further increases, the total reconstruction time may increase. This is because more measurements are required for exact recovery. However, the total reconstruction time, and the average and the worst reconstruction time of the parallel CS reconstruction are much less than those of the centralized CS reconstruction.

IV. CONCLUSION

The permutation enhanced parallel reconstruction architecture for CS has been proposed, where all segments of the projection are reconstructed in parallel, and the error performance is enhanced by permutation. It has been shown that via parallel CS reconstruction, the computational complexity and the reconstruction time can be reduced significantly, with a certain degree of error performance degradation. Permutation has been employed to reduce the minimum number of measurements required for exact reconstruction in the parallel CS reconstruction architecture. It has been further demonstrated that permutation can be implicitly performed via exploiting a new measurement matrix which is the product of the block diagonal sensing matrix, the permutation matrix, and the transpose of the sparsifying basis.

Hence, the encoder acts as a linear system, and it enables to use the proposed permutation enhanced parallel reconstruction with a linear CS sampling device such as the single-pixel camera.

REFERENCES

- [1] D. L. Donoho, “Compressed sensing,” *IEEE Trans. Inf. Theory*, vol. 52, no. 4, pp. 1289–1306, Apr. 2006.
- [2] E. J. Candès, “Compressive sampling,” in *Proc. Int. Cong. Math.*, Madrid, Spain, Aug. 22–30, 2006, pp. 1433–1452.
- [3] L. Gan, “Block compressed sensing of natural images,” in *Proc. Int. Conf. Digital Signal Process.*, Cardiff, UK, Jul. 1–4, 2007, pp. 403–406.
- [4] L. Gan, T. T. Do, and T. D. Tran, “Fast compressive imaging using scrambled block Hadamard ensemble,” in *Proc. 16th European Signal Process. Conf.*, Lausanne, Switzerland, Aug. 25–29, 2008.
- [5] M. F. Duarte and R. G. Baraniuk, “Kronecker compressive sensing,” *IEEE Trans. Image Process.*, vol. 21, no. 2, pp. 494–504, Feb. 2012.
- [6] H. Fang, S. A. Vorobyov, H. Jiang, and O. Taheri, “2D signal compression via parallel compressed sensing with permutations,” in *Proc. 46th Annual Asilomar Conf. Signals, Systems, and Computers*, Pacific Grove, California, USA, Nov. 4–7, 2012, pp. 1925–1929.
- [7] ———, “Permutation meets parallel compressed sensing: How to relax restricted isometry property for 2D sparse signals,” *IEEE Trans. Signal Process.*, vol. 62, no. 1, pp. 196–210, Jan. 2014.
- [8] M. F. Duarte, M. A. Davenport, D. Takhar, J. N. Laska, T. Sun, K. F. Kelly, and R. G. Baraniuk, “Single-pixel imaging via compressive sampling,” *IEEE Signal Process. Mag.*, vol. 25, no. 2, pp. 83–91, Mar. 2008.
- [9] E. J. Candès and T. Tao, “Decoding by linear programming,” *IEEE Trans. Inf. Theory*, vol. 51, no. 12, pp. 4203–4215, Dec. 2005.
- [10] S. Boyd and L. Vanderberghe, *Convex Optimization*. New York: Cambridge Univ. Press, Dec. 2008.
- [11] S. Pudlewski, T. Melodia, and A. Prasanna, “Compressed-sensing-enabled video streaming for wireless multimedia sensor networks,” *IEEE Trans. Mobile Comput.*, vol. 11, no. 6, pp. 1060–1072, Jun. 2012.
- [12] A. Averbuch, S. Dekel, and S. Deutsch, “Adaptive compressed image sensing using dictionaries,” *SIAM J. Imag. Sci.*, vol. 5, no. 1, pp. 57–89, 2012.